

Nonlinear Cross-Phase Modulation with Intense Single-Cycle Terahertz Pulses

Y. Shen,¹ T. Watanabe,¹ D. A. Arena,¹ C.-C. Kao,¹ J. B. Murphy,¹ T. Y. Tsang,² X. J. Wang,¹ and G. L. Carr¹

¹*National Synchrotron Light Source, Brookhaven National Laboratory, Upton, New York 11973-5000, USA*

²*Instrumentation Division, Brookhaven National Laboratory, Upton, New York 11973-5000, USA*

(Received 27 December 2006; published 23 July 2007)

We have demonstrated nonlinear cross-phase modulation in electro-optic crystals using intense, single-cycle terahertz (THz) radiation. Individual THz pulses, generated by coherent transition radiation emitted by subpicosecond electron bunches, have peak energies of up to 100 μJ per pulse. The time-dependent electric field of the intense THz pulses induces cross-phase modulation in electro-optic crystals through the Pockels effect, leading to spectral shifting, broadening, and modulation of copropagating laser pulses. The observed THz-induced cross-phase modulation agrees well with a time-dependent phase-shift model.

DOI: [10.1103/PhysRevLett.99.043901](https://doi.org/10.1103/PhysRevLett.99.043901)

PACS numbers: 42.65.-k, 41.75.Ht

The generation of coherent terahertz (THz) radiation from subpicosecond relativistic electron bunches has been demonstrated over the past few years [1–5]. The coherent superposition of the radiated fields from such ultrashort electron bunches dramatically enhances the emitted energy, peak power, and peak electric field of THz pulses, which can be orders of magnitude higher than that produced by photoconductive switches and optical rectification in electro-optic crystals. Since the THz pulse emitted by a subpicosecond electron bunch results in one oscillation cycle of electromagnetic radiation, accelerator-based intense THz sources offer unique opportunities for studying novel nonlinear optical phenomena in the single-cycle regime.

Relativistic electron beams can be used to produce coherent THz radiation through a variety of radiation mechanisms such as synchrotron radiation from a bending magnet [1–3], transition radiation from the interface between different refractive index media [5,6], diffraction radiation from slits or apertures [7], Cherenkov radiation from a solid dielectric [8], and Smith-Purcell radiation from a periodic structure [9]. Coherent radiation occurs at wavelengths longer than, or comparable to, the bunch length of the electron beam, with an intensity that scales with N^2 , where N is the number of electrons in the bunch, and typically ranges from $\sim 10^8$ – 10^9 for an electron accelerator. The radiation pulse created by such a bunch can be subpicosecond in time and therefore contains coherent spectral content up to a few THz. Coherent transition radiation at millimeter and submillimeter wavelengths using relativistic electrons was observed over a decade ago [6]. Recently, it was used to generate THz radiation from a laser-accelerated relativistic electron beam [5]. In this Letter, we report the production and characterization of ~ 100 μJ single-cycle coherent THz radiation pulses from a linear accelerator in the form of coherent transition radiation. To our knowledge, this is the highest energy ever achieved to date in a single-cycle THz pulse. We also demonstrate that the strong electric field associated with intense THz radiation can induce nonlinear cross-

phase modulation (XPM) in an electro-optical crystal through the Pockels effect. XPM is the optical phase change of an electromagnetic wave due to the interaction with another wave in a nonlinear medium. This phenomenon has been extensively studied via the third-order optical Kerr effect, in which the phase change of a weak probe is proportional to the intensity of a strong excitation pulse, usually containing many oscillation cycles of optical fields [10]. In contrast, we show that an intense single-cycle THz pulse can induce second-order nonlinear XPM via its strong electric field through the Pockels effect, leading to spectral shifting, broadening, and modulation of copropagating near-infrared laser pulses.

The intense THz source described here has been developed at the Source Development Lab of Brookhaven National Laboratory (BNL). This accelerator-based facility [11] consists of a 1.6 cell photoinjector, four SLAC-type linac sections, and a 4-dipole chicane bunch compressor. The photocathode rf gun is illuminated by a frequency-tripled Ti:sapphire laser amplifier at 266 nm, producing ~ 5 ps (FWHM) electron bunches with ~ 500 pC charge and 2.5 Hz repetition rate. The electrons are accelerated to 120 MeV, with one linac section producing a longitudinal energy chirp that, in combination with the chicane, compresses the bunches to below 1 ps. At this time scale, coherent spectral content up to a few THz is expected. After passing through the linac, the electron beam is incident onto a 2 cm diameter aluminum mirror that generates the transition radiation (both coherent and incoherent). The coherent THz radiation is extracted from the accelerator vacuum pipe through a z -cut crystalline quartz window, and the pulse energy is measured with a calibrated pyroelectric detector (Model J4-5, Molelectron), which has a reasonably flat spectral response. Pulse energies in excess of 50 μJ are observed, consistent with estimates using the angle-integrated Ginzburg-Frank formula [12] for a 500 pC electron bunch ($\sim 3 \times 10^9$ electrons) radiating coherently up to ~ 1 THz. Pulse energies as high as 100 μJ have been measured when the charge approaches ~ 1 nC. An $f/1.5$, 90° off-axis parabolic mirror focuses the ~ 100 μJ THz

radiation down to a ~ 3 mm spot size. An estimate of the electric field strength associated with such a THz pulse is $\sim 7 \times 10^7$ V/m, i.e., approaching 1 MV/cm.

We attempted to measure the THz temporal E field of these intense pulses by single-shot electro-optic (EO) sampling with chirped laser pulses [13]. A small fraction of the Ti:sapphire laser output is used as a probe, which is chirped by a grating stretcher. This linearly polarized probe pulse and the THz pulse are copropagated through a [110]-oriented ZnTe crystal with the probe continuing through a quarter wave plate and a polarizer analyzer. The time evolution of the THz E field is transformed into an intensity modulation on the probe spectrum. The probe transmission is given by $T = (1 + \sin\Gamma)/2$ where $\Gamma = \pi E_{\text{THz}}(t)L/V_{\lambda/2}$ is the phase retardation experienced by the probe when propagating through the length L of an EO crystal, $V_{\lambda/2}$ is the half-wave voltage ($V_{\lambda/2} = 3 \times 10^3$ V for ZnTe at 795 nm). Note that T varies linearly with the applied THz field strength E_{THz} only when $\Gamma \ll 1$. However, for a ~ 50 μJ THz pulse focused down to a ~ 3 mm spot size, we estimate $E_{\text{THz}} \approx 5.2 \times 10^7$ V/m, leading to $\Gamma \approx 9\pi$ for 0.5 mm thick ZnTe. Such a strong THz E field will “over-rotate” the induced birefringence and cause the linear EO sampling method to break down. Indeed, distortion of the measured THz waveform is observed when the THz pulse energy exceeds ~ 1 μJ . To avoid these distortions, a meshed wire attenuator is used to reduce THz energy on the ZnTe crystal to ~ 0.3 μJ . Figure 1(a) shows the spectral profiles of the chirped (3 mm/ps) probe pulse with and without the presence of the THz field. The retrieved single-cycle THz waveform is shown in Fig. 1(b). Figure 1(c) is the power spectrum of the waveform depicted in Fig. 1(b). The dc component in the derived spectral intensity can be attributed to the apodization used to reduce noise from data acquisition as well as structure from atmospheric absorption. The power spec-

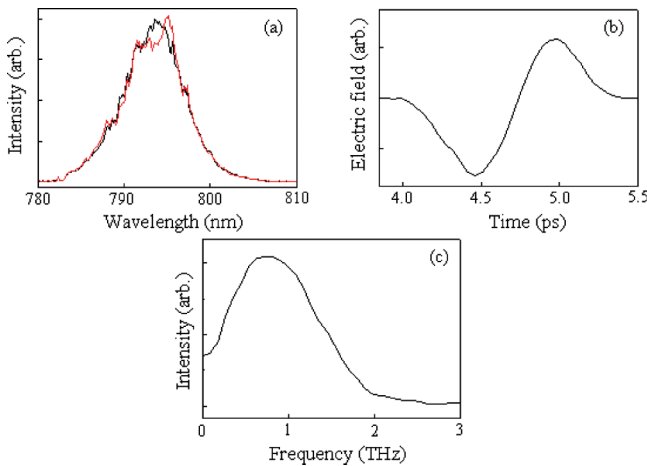


FIG. 1 (color). (a) Raw data, single-shot probe pulse spectra with (red) and without (black) a copropagating THz pulse, (b) measured single-shot THz waveform, and (c) Fourier transform of the waveform of (a).

trum for this single-cycle pulse reaches up to 2 THz and peaks near 1 THz.

At the higher THz field strengths we observe that the time-dependent Pockels EO effect is sufficiently strong to produce cross-phase modulation of the copropagated laser pulse. To illustrate this, consider an intense THz pulse and a weak laser probe pulse, of complex amplitude E_{THz} and E_{probe} , respectively, copropagating through an EO crystal. The change in refractive index seen by the probe can be expressed as [14] $n = n_0 + \Delta n_1 + \Delta n_2$, where n_0 is the linear refractive index of the EO crystal, and $\Delta n_1 = \chi^{(2)} E_{\text{THz}}/n_0$ and $\Delta n_2 = 3\chi^{(3)} |E_{\text{THz}}|^2/(2n_0)$ are the changes in the refractive index induced by Pockels and Kerr effects, respectively. For ZnTe [15], second-order susceptibility $\chi^{(2)} = 9.0 \times 10^{-11}$ m/V and third-order susceptibility $\chi^{(3)} = 3 \times 10^{-19}$ m²/V². With $E_{\text{THz}} = 5 \times 10^7$ V/m, $\Delta n_2/\Delta n_1 \approx 0.2$, indicating that the refractive index change in ZnTe is dominated by Pockels effect when $E_{\text{THz}} < 5 \times 10^7$ V/m. This refractive index change affects the phase of the probe, resulting in a total (integrated) phase shift $\Delta\varphi(t)$ of [10]

$$\Delta\varphi(t) = (2\pi/\lambda_0) \int_0^L \Delta n[E_{\text{THz}}(t - \beta z)] dz \quad (1)$$

where λ_0 is the central wavelength of the probe pulse, and β is a walk-off parameter.

For the moment we will ignore walk-off effects, in which case the phase shift is directly proportional to the THz E field, i.e., $\Delta\varphi(t) = (2\pi L/\lambda_0)\chi^{(2)} E_{\text{THz}}(t)/n_0$. When the probe pulse is short compared to the time variation of the THz waveform, it is insightful to expand the phase shift in a Taylor series,

$$\begin{aligned} \Delta\varphi(t) &= \varphi(t_0) + \left. \frac{d\varphi}{dt} \right|_{t_0} (t - t_0) + \left. \frac{1}{2} \frac{d^2\varphi}{dt^2} \right|_{t_0} (t - t_0)^2 + \dots \\ &\propto E_{\text{THz}}(t_0) + \left. \frac{dE_{\text{THz}}}{dt} \right|_{t_0} (t - t_0) + \left. \frac{1}{2} \frac{d^2E_{\text{THz}}}{dt^2} \right|_{t_0} \\ &\quad \times (t - t_0)^2 + \dots \end{aligned} \quad (2)$$

where $t - t_0$ is limited to the temporal extent of the probe pulse, relative to the THz E field at time t_0 . The first term is the conventional Pockels phase shift commonly used for coherent THz detection. Since the instantaneous probe frequency is given by $\omega(t) = \omega_0 - d\Delta\varphi(t)/dt$, where ω_0 is the carrier frequency of probe, the second term in phase expansion describes a frequency shift of the probe while the third term describes a linear chirp. Though these effects can all take place simultaneously, they tend to occur separately for a single-cycle oscillation; e.g., the second (t -linear) term is large near the central zero crossing of the THz pulse while the 1st and 3rd terms are close to zero. The frequency shift is reduced when walk-off is included, and can be illustrated by considering a bipolar transient THz pulse with central frequency $\Omega_0 = 1$ THz and E field waveform shown in the inset of Fig. 2. We assume a 30 μJ THz pulse focused down to a 3 mm diameter spot

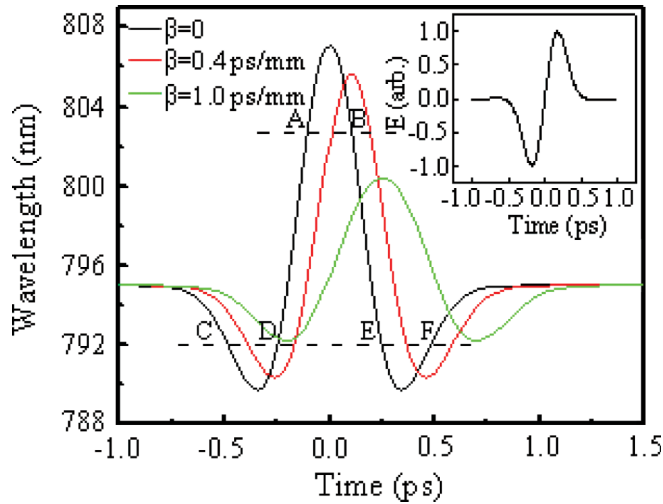


FIG. 2 (color). Calculated THz-field-induced wavelength shift through XPM in ZnTe. The inset displays the single-cycle bipolar THz pulse at 1 THz.

to yield a maximum E field of 3.5×10^7 V/m, noting that the Pockels effect dominates over the Kerr effect (which is subsequently neglected). Figure 2 shows the THz-induced wavelength shift of the probe (incident wavelength $\lambda_0 = 795$ nm) as a result of Pockels XPM in the ZnTe (thickness $L = 0.5$ mm) calculated as a function of the delay time between the THz and probe waveforms, and for different walk-off parameters.

Notice that, as the probe is scanned through the THz E field, the probe's center frequency shifts up and down, yielding a large redshift (or blueshift) when the probe overlaps the central zero-crossing of the THz E field, and two blueshifts (or redshifts) at the leading and trailing edges, respectively, as shown in Fig. 2. With perfect group-velocity matching ($\beta = 0$), the probe continues to interact with the same segment of the THz pulse during its propagation in the EO crystal and the accumulated phase shift increases linearly with the crystal length. However, with imperfect group-velocity matching ($\beta \neq 0$), the probe pulse slips across different portions of THz E field

such that the effect becomes degraded. The calculated β is 1.05 ps/mm, and the measured value is 0.4 ps/mm [16]. Because of this walk-off effect, the wavelength (frequency) shift that the probe accumulates is considerably smaller. This is illustrated in Fig. 2, where the frequency shifts are reduced by $\sim 50\%$ for $\beta = 1.0$ ps/mm.

The temporal variation of accumulated phase not only leads to a frequency shift but also introduces spectral broadening of the probe in the form of a linear chirp (3rd term in phase expansion). The maximum broadening occurs near the crests and troughs of the THz E field, and is given by $\Delta\omega_{\max} = \Delta\varphi_{\max}/T_0$, where T_0 is the probe pulse duration, and $\Delta\varphi_{\max}$ is the maximum phase shift obtained with Eq. (2). For a ~ 120 fs probe pulse, it is estimated that the maximum spectral broadening $\Delta\lambda_{\max} \approx 15$ nm with $E_{\text{THz}} = 3.5 \times 10^7$ V/m and $\beta = 0$; however, $\Delta\lambda_{\max}$ is reduced to ~ 8 nm with $\beta = 1.0$ ps/mm.

We next consider the situation when the initial laser probe itself is stretched to a length somewhat longer than the THz pulse prior to mixing in the ZnTe. When the laser probe overlaps with the THz, XPM induces new instantaneous frequencies at different time points of the probe. As shown in Fig. 2 (black curve), instantaneous frequencies at different time points of the probe, $\omega(t) = \omega_0 - d\Delta\varphi(t)/dt$, are identical at points A and B or points C, D, E, and F. The power spectrum attributed to points A and B is proportional to $I(\omega) = |E_A(\omega)|^2 + |E_B(\omega)|^2 + 2|E_A(\omega)||E_B(\omega)|\cos(\varphi_A - \varphi_B)$. Depending on the relative phase difference, $\varphi_A - \varphi_B$, the frequency pairs can interfere constructively or destructively. The resulting spectral intensity is more complicated when the EO setup with polarization analysis is used. Under these circumstances, extracting the underlying THz waveform becomes extremely difficult and of course the standard interpretation in terms of the quasistatic EO effect breaks down completely.

Experiments are performed to illustrate the THz-induced spectral shift, broadening, and modulation. In our first study, a ~ 120 fs (FWHM), 795 nm pulse from the Ti:sapphire laser amplifier acts as a probe, and a

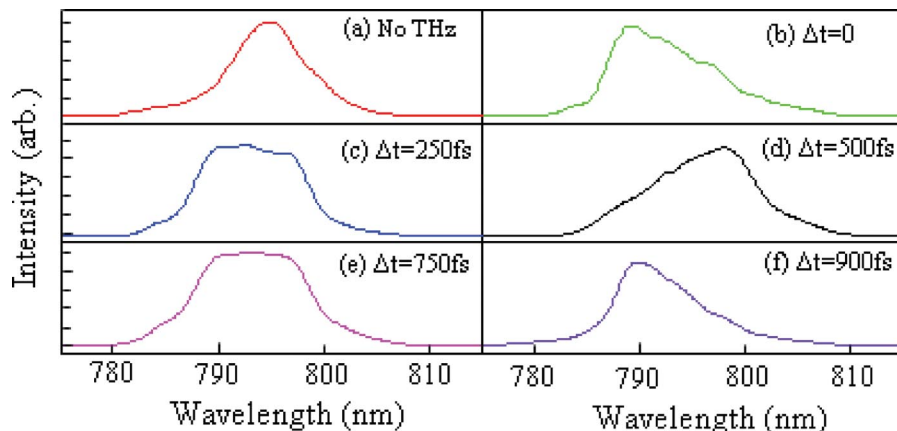


FIG. 3 (color). THz-field-induced spectral shift and broadening of a 120 fs 795 nm probe pulse.

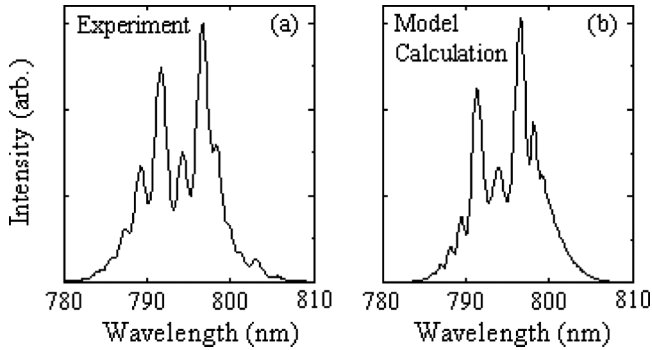


FIG. 4. Single-cycle THz-induced EO signal using a chirped pulse; (a) measurement and (b) model calculation.

$\sim 30 \mu\text{J}$ THz pulse is focused into a 0.5 mm thick ZnTe crystal with ~ 3 mm spot size to induce XPM. The corresponding E field strength at the ZnTe crystal is estimated to be $\sim 3.5 \times 10^7$ V/m; therefore, the XPM is dominated by the Pockels effect as calculated above. The experimental arrangement is similar to that used for conventional EO measurements of low intensity THz waveforms, except that there is no quarter wave plate and no polarizer analyzer after the ZnTe. Also, the THz and laser polarizations were oriented to produce the simplest phase modulation ($E_{\text{probe}} \parallel [110]$, $E_{\text{THz}} \perp [110]$) [17]. By varying the time delay between THz and probe, the probe interacts with different parts of the THz E field, and the probe spectrum from each interaction is measured with a spectrometer. No spectral modulation is observed when the THz is not present, as shown in Fig. 3(a), which indicates the probe is weak and does not exhibit self-phase modulation (SPM). Figures 3(b)–3(f) show probe spectra as a function of the time delay between the THz and probe pulses. Two blueshifts and one redshift are observed as the probe is scanned across the THz field. The central wavelength of the probe is shifted as much as ~ 5 nm toward the blue side [Figs. 3(b) and 3(f)] and ~ 4 nm toward the red [Fig. 3(d)]. Further, the probe spectrum is broadened by a factor of ~ 1.5 at the crest and trough of the THz E field [Figs. 3(c) and 3(e)]. The measured spectral shift and broadening are compatible with the walk-off parameter of 1 ps/mm. The crest-trough asymmetry of the THz waveform (the trough to crest ratio is $\sim 4:5$, as shown in Fig. 1) reduces the redshift, and leads to less blueshift at the trailing edge of THz E field, as shown in Fig. 3. The XPM-induced spectral shift and broadening depends on the strength of THz E field, which becomes negligible when the THz pulse energy is below $1 \mu\text{J}$.

In the second experiment, a 2 ps (FWHM) chirped pulse from the Ti:sapphire laser serves as a probe and copropagates with a THz pulse through the ZnTe crystal in the conventional EO sampling setup. When the THz and the probe overlap in time, THz-induced XPM produces spectral shifting such that components with the same instantaneous frequency but different phase interfere construc-

tively or destructively. This, plus the intensity modulation from the polarization analysis, yields the complex probe spectrum shown in Fig. 4. This also illustrates how the conventional interpretation of an electro-optic signal would fail to yield the proper single-cycle THz waveform. Also shown is a representative model calculation based on a single-cycle THz pulse with a E field strength of 2.5×10^7 V/m, illustrating similarly complex structure.

In summary, we have generated and characterized $\sim 100 \mu\text{J}$ single-cycle THz radiation through coherent transition radiation. We have shown that the accelerator-based THz source can produce sufficient E field strength to open up the field of nonlinear optics with single-cycle THz pulses. We have demonstrated that the intense THz radiation can induce XPM effect, giving rise to spectral shifting and broadening of a copropagated laser pulse. The THz-induced XPM effect has important features that can be used to control the spectral, temporal, and spatial properties of ultrashort laser pulses. For example, in the temporal domain, THz-induced XPM imposes a frequency chirp across the copropagating pulse, which could allow for optical pulse compression. In the spatial domain, the strong THz-induced XPM effect can produce a dynamic lensing effect [18], which can be used to deflect a copropagating laser beam.

This work is supported by the Office of Naval Research under Contract No. N0002405MP70325, U.S. Department of Energy under Contract No. DE-AC02-98CH10886, and BNL Laboratory Directed R&D funds. The authors gratefully acknowledge enlightening discussions with J. Misewich, T. Heinz, and D. Reitze. We also wish to thank P. Singh, G. Nintzel, and A. Woodhead for technical assistance.

-
- [1] G.L. Carr *et al.*, Nature (London) **420**, 153 (2002).
 - [2] J.M. Byrd *et al.*, Phys. Rev. Lett. **89**, 224801 (2002).
 - [3] M. Abo-Bakr *et al.*, Phys. Rev. Lett. **88**, 254801 (2002).
 - [4] A. Doria *et al.*, Phys. Rev. Lett. **93**, 264801 (2004).
 - [5] W.P. Leemans *et al.*, Phys. Rev. Lett. **91**, 074802 (2003).
 - [6] Y. Shibata *et al.*, Phys. Rev. A **45**, R8340 (1992).
 - [7] Y. Shibata *et al.*, Phys. Rev. E **52**, 6787 (1995).
 - [8] T. Takahashi *et al.*, Phys. Rev. E **62**, 8606 (2000).
 - [9] S.E. Korbly *et al.*, Phys. Rev. Lett. **94**, 054803 (2005).
 - [10] G.P. Agrawal, *Nonlinear Fiber Optics* (Academic Press, London, 2001), 3rd ed.
 - [11] A. Doyuran *et al.*, Phys. Rev. ST Accel. Beams **7**, 050701 (2004).
 - [12] U. Happek *et al.*, Phys. Rev. Lett. **67**, 2962 (1991).
 - [13] Z. Jiang and X.-C. Zhang, Appl. Phys. Lett. **72**, 1945 (1998); I. Wilke *et al.*, Phys. Rev. Lett. **88**, 124801 (2002).
 - [14] R.W. Boyd, *Nonlinear Optics* (Academic Press, London, 2003), 2nd ed.
 - [15] J.-P. Caumes *et al.*, Phys. Rev. Lett. **89**, 047401 (2002).
 - [16] Q. Wu *et al.*, Appl. Phys. Lett. **68**, 2924 (1996).
 - [17] S. Casalbuoni *et al.*, TESLA Report No. 2005-01.
 - [18] A. Schneider *et al.*, Appl. Phys. Lett. **84**, 2229 (2004).